UC Davis
UC Davis Previously Published Works

Title

RNA-binding Protein PCBP2 Regulates p73 Expression and p73-dependent Antioxidant Defense*

Permalink

Journal

ISSN

Authors

Ren, Cong
Zhang, Jin
Yan, Wensheng
et al.

Publication Date

DOI

Peer reviewed

RNA-binding Protein PCBP2 Regulates p73 Expression and p73-dependent Antioxidant Defense*[S]

Cong Ren[1,2], Jin Zhang[1,3], Wensheng Yan, Yanhong Zhang, and Xinbin Chen[4]

From the Comparative Oncology Laboratory, Schools of Medicine and Veterinary Medicine, University of California, Davis, California 95616

TAp73, a member of the p53 family tumor suppressors, plays a critical rule in tumor suppression and neuronal development. However, how p73 activity is controlled at the posttranscriptional level is not well understood. Here, we showed that TAp73 activity is regulated by RNA-binding protein PCBP2. Specifically, we found that knockdown or knock-out of PCBP2 reduces, whereas ectopic expression of PCBP2 increases, TAp73 expression. We also showed that PCBP2 is necessary for p73 mRNA stability via the CU-rich elements in p73 3′-UTR. To uncover the biological relevance of PCBP2-regulated TAp73 expression, we showed that ectopic expression of PCBP2 inhibits, whereas knockdown or knock-out of PCBP2 increases, the production of reactive oxygen species (ROS) in a TAp73-dependent manner. Additionally, we found that glutaminase 2 (GLS2), a modulator of p73-dependent antioxidant defense, is also involved in PCBP2-regulated ROS production. Moreover, we generated PCBP2-deficient mice and primary mouse embryonic fibroblasts (MEFs) and showed that loss of PCBP2 leads to decreased p73 expression and, subsequently, increased ROS production and accelerated cellular senescence. Together, our data suggest that PCBP2 regulates p73 expression via mRNA stability and p73-dependent biological function in ROS production and cellular senescence.

p73, along with p53 and p63, consists of the p53 family and is expressed as multiple isoforms (1). Through alternative splicing, at least seven isoforms (α, β, γ, δ, ϵ, ζ, and η) are expressed. In addition, due to the usage of two different promoters, p73 is expressed as two different isoforms, TAp73 and ΔNp73. The TAp73 isoform is transcribed from the upstream P1 promoter and contains an N-terminal activation domain conserved in p53, whereas the ΔNp73 isoform is produced by the downstream P2 promoter and, thus, N-terminally truncated. Consequently, TAp73, like p53, regulates an array of genes for tumor suppression (2). Indeed, mice deficient in TAp73 are prone to spontaneous tumors and premature aging (3, 4). By contrast, ΔNp73 acts as an oncoprotein against TAp73 as well as p53 (5,

6). For example, ΔNp73 promotes cell immortalization in mouse embryonic fibroblasts (MEFs)[5] and cooperates with oncogenic Ras in cell transformation in vitro and in vivo (7). In addition, mice deficient in ΔNp73 do not develop tumors but exhibit delayed onset of moderate neurodegeneration (8, 9). The opposing functions of TAp73 and ΔNp73 create more complicated issues for the role of p73 in cancer. Therefore, it is important to understand how p73 expression is controlled, which would advance our understanding of p73 biology and shed light on the development of novel strategy for cancer management.

The poly(rC)-binding protein 2 (PCBP2) is a RNA-binding protein and belongs to the PCBP family. Members of PCBP family are characterized by their affinity to single-stranded poly(C) motifs in their target mRNAs (10). PCBP2 is a multifunctional protein and regulates gene expression at multiple levels including mRNA metabolism and translation. For example, PCBP2 regulates mRNA stability of α-globin (11) and FHL3 (12) and mRNA translation of p21 (13) and c-myc (14). Additionally, PCBP2 is found to regulate RNA replication and mRNA translation of several RNA viruses, including poliovirus (15), coxsackievirus (16), and rhinovirus (17). Interestingly, apart from its RNA binding activity, PCBP2 can function as an iron chaperone and, thus, regulate iron homeostasis by delivering iron to ferritin (19), deoxyhypusine hydroxylase (20), prolyl hydroxylase (21), and asparaginyl hydroxylase (21). Notably, studies suggest that PCBP2 is involved in tumor development. For instance, PCBP2 expression is found to be high in leukemia and glioma (12, 22) but low in oral cancer (23). However, the role of PCBP2 in tumorigenesis is not clear.

To better understand the role of p73 in cancer, we aim to identify a novel regulator of p73 and understand how p73 biological activity is modulated by the regulator. To this end we performed a pilot study to determine whether p73 expression is regulated by several RNA-binding proteins including PCBP2. Indeed, we found that TAp73 expression is regulated by PCBP2 via mRNA stability. We also found that PCBP2 modulates the activity of TAp73 to regulate the production of reactive oxygen species (ROS) and cellular senescence.

Materials and Methods

Cell Culture and Cell Line Generation—Human non-small cell lung carcinoma cell line H1299, human colon cancer cell

---

[S] This article contains supplemental Table 1.
[1] Both authors contributed equally to this work.
[2] Present address: School of Biotechnology, Jiangnan University, Wuxi, Jiangsu 214122, China.
[3] To whom correspondence may be addressed. E-mail: jinzhang@ucdavis.edu.
[4] To whom correspondence should be addressed. E-mail: xbchen@ucdavis.edu.

[5] The abbreviations used are: MEF, mouse embryonic fibroblast; PCBP2, poly(rC)-binding protein 2; ROS, reactive oxygen species; REMSA, RNA electrophoretic mobility shift assay; SA-β-gal, senescence-associated β-galactosidase; GLS2, glutaminase-2; qRT, quantitative real-time.

line p53$^{-/-}$ HCT116, human pancreatic cancer cell line MIA-PaCa2, and human colon adenocarcinoma cell line SW480 were cultured in DMEM (Invitrogen) with 10% fetal bovine serum (HyClone) and maintained at 37 °C in 5% CO_2 incubator. MEFs were cultured in DMEM supplemented with 10% FBS plus 1× nonessential amino acids (HyClone) and 55 μM β-mercaptoethanol. To generate PCBP2 or TAp73 knock-out cell lines, plasmid expressing *Streptococcus pyogenes* Cas9 (spCas9) along with a sgRNA targeting the *PCBP2* gene or *TAp73* gene was transfected into cells using Metafectene Pro reagent (Biontex Laboratories) followed by puromycin selection for 3 weeks. The loss of *PCBP2* or *TAp73* was verified by Western blot analysis.

Plasmids—To generate pcDNA3 vector expressing human PCBP2, the full-length human PCBP2 gene was amplified using cDNAs from H1299 cells with an upstream primer, PCBP2-1-HindIII-F, and a downstream primer, PCBP2–1451-XhoI-R. The PCR products were cloned into pcDNA3 and then confirmed by sequencing. To generate pGEX-4T-1 vector expressing recombinant human PCBP2, the same strategy was used except that PCBP2-EcoRI-F was used as upstream primer and PCBP2-XhoI-R was used as downstream primer. To generate a vector expressing sgRNA targeting the *PCBP2* gene and *TAp73* gene, DNA oligos were annealed and inserted into vector pSpCas9(BB)-2A-puro (Addgene plasmid #48139) through BbsI sites as previously described (24). The primers are listed in supplemental Table 1. pcDNA3 vector expressing HA-tagged TAp73α was generated previously (25). The luciferase reporters, pGL3-p73 3′-UTR-A′ and pGL3-p73 3′-UTR-A′(ΔCU1), were generated previously (26).

RNA Interference—Scrambled siRNA (GGC CGA UUG UCA AAU AAU U) or siRNA against PCBP2 (CCU CUA GAG GCC UAU ACC A) (27) were synthesized by Dharmacon (GE Healthcare). To knock down PCBP2, 50 nM siRNA was transfected into cells using Metafectene Pro reagent according to the user's manual.

Antibodies and Western Blot Analysis—The antibodies used in this study were anti-PCBP2 antibody (23-G, Santa Cruz Biotechnology), anti-p73 (A300, Bethyl Laboratories), anti-actin antibody (A2066, Sigma), and mouse IgG (I5381, Sigma). For Western blot analysis, whole cell lysates were prepared with 2×SDS sample buffer, separated in 8–12% SDS-PAGE, transferred to nitrocellulose membrane, and then probed with the indicated antibodies. The protein bands were visualized by the enhanced chemiluminescence using the ChemiDoc-It imaging system (UVP, Upland, CA). The level of protein was quantified by densitometry using the ImageJ program (UVP).

RNA Isolation, RT-PCR Analysis, and Quantitative PCR—Total RNAs were extracted from cells using TRIzol reagent (Invitrogen) according to the user's manual. For RT-PCR analysis, cDNA was synthesized using RevertAid Reverse Transcriptase (Thermo) followed by PCR. The PCR program used for amplification was (i) 94 °C for 5 min, (ii) 94 °C for 45 s, (iii) 60 °C for 45 s, (iv) 72 °C for 1 min, and (v) 72 °C for 10 min. From steps 2–4, the cycle was repeated 25 times for actin or 32 times for TAp73. For quantitative PCR, reactions were prepared with Maxima SYBR Green qPCR Master Mix (Thermo) and then run on a real-time PCR system (Mastercycler ep realplex, Eppen-dorf, Germany) using a three-step cycling program: 95 °C for 15 min followed by 40 cycles of 95 °C for 15 s, 53 °C (for mouse actin), or 60 °C (for all other genes) for 30 s, and 72 °C for 20 s. A melting curve (57–95 °C) was generated at the end of each run to verify the specificity. The relative level of transcripts was calculated upon normalization to that of actin. The primers used for PCR are listed in supplemental Table 1.

RNA Immunoprecipitation Assay—The RNA-Chip assay was performed as previously described (28). Briefly, cell lysates were immunoprecipitated with 2 μg of anti-PCBP2 or isotype control IgG at 4 °C overnight. The RNA-protein immunocomplexes were brought down by protein A/G beads (Sigma) followed by RT-PCR analysis.

RNA Electrophoretic Mobility Shift Assay (REMSA)—Recombinant proteins were expressed in bacteria BL21 (DE3) and purified by glutathione-Sepharose beads. RNA probes were generated and ^{32}P-labeled by *in vitro* transcription using PCR products containing T7 (GGA TCC TAA TAC GAC TCA CTA TAG GGA G) promoter and various regions from TAp73α 5′ or 3′-UTR as a template. The primers to amplify various probes are listed in supplemental Table 1. REMSA were performed as previously described (29). Briefly, ^{32}P-labeled probes were incubated with recombinant protein in a binding buffer (10 mM HEPES-KOH at pH 7.5, 90 mM potassium acetate, 1.5 mM magnesium acetate, 2.5 mM DTT, 40 units of RNase inhibitor) at 25 °C for 30 min. The RNA-protein complexes were resolved on a 5% acrylamide gel, and radioactive signals were detected by autoradiography.

Luciferase Assay—Luciferase assay was performed as previous described (30). Briefly, cells were transfected with 5 ng of Renilla luciferase vector (pRL-CMV; Promega, Madison, WI) and 250 ng of a pGL3 reporter vector. 24 h post transfection, luciferase activity was measured by the dual luciferase kit (Promega) using the Turner Designs luminometer (Turner Designs, Sunnyvale, CA). Triplicate samples were used, and the relative luciferase activity is a relative -fold change over the luciferase activity of pGL3 control vector in control cells.

Isolation of Primary MEFs—PCBP2 heterozygous mice were generated by University of California, Davis mouse program with JM8A3.N1 ES cells. To generate *PCBP2*$^{-/-}$ MEFs, *PCBP2* heterozygous mice were bred, and MEFs were isolated from 13.5-day-old (E13.5) embryos as previously described (31). All animals used in this study were housed at the Teaching and Research Animal Care Services (TRACS) Husbandry facilities at the University of California, Davis. The use of animals and protocols were approved by the Institutional Animal Care and Use Committee (IACUC) at the University of California, Davis.

Senescence-associated β-Galactosidase (SA-β-gal) Staining—MEFs at passage 4 were seeded into 6-well plates followed by a 1-day culture and stained for SA-β-gal as previously described (32).

ROS Measurement—The level of ROS was determined by using 2′,7′-dichlorofluorescin diacetate as previously reported (33). Briefly, cells were washed with PBS and stained for 15 min with 20 μM 2′,7′-dichlorofluorescin diacetate (Sigma) in Hanks' balanced salt solution. The cells were trypsinized and then resuspended in Hanks' balanced salt solution in a well of a 96-well plate followed by fluorescence measurements using
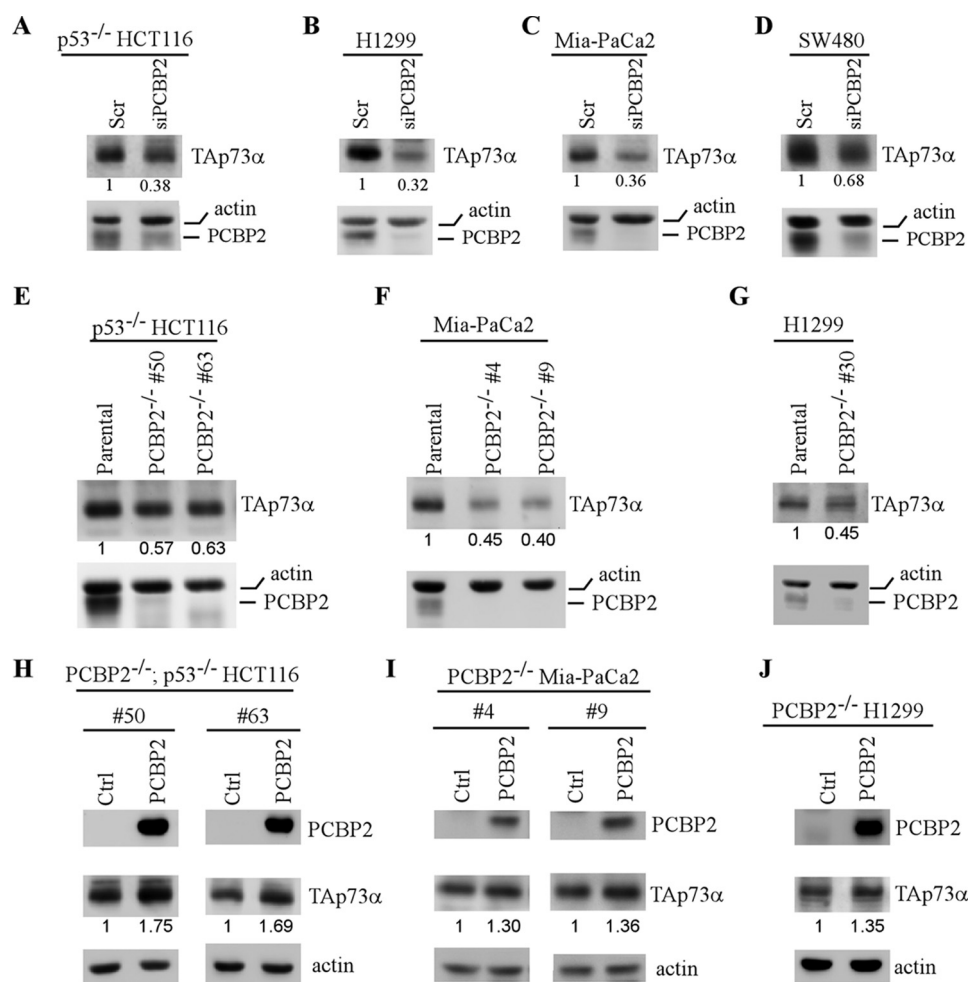
FIGURE 1. **Knock-out or knockdown of PCBP2 decreased, whereas ectopic expression of PCBP2 increased TAp73 expression.** *A–D*, p53$^{-/-}$ HCT116 (*A*), H1299 (*B*), Mia-PaCa2 (*C*), and SW480 (*D*) cells were transfected with a scrambled (*Scr*) or PCBP2 (*SiPCBP2*) siRNA for 3 days, and the level of TAp73α, PCBP2, and actin was determined by Western blot analysis. The basal levels of TAp73α were arbitrarily set at 1.0, and the -fold change is shown *below each lane*. *E–G*, the levels of TAp73α, PCBP2, and actin were measured in parental and PCBP2-KO p53$^{-/-}$ HCT116 (*E*), Mia-PaCa2 (*F*), and H1299 (*G*) cells. The basal levels of TAp73α were arbitrarily set at 1.0, and the fold change is shown *below each lane*. *H–J*, PCBP2-KO p53$^{-/-}$ HCT116 (*H*), Mia-PaCa2 (*I*), and H1299 (*J*) cells were transiently transfected with a control or PCBP2-expressing vector for 24 h, and the levels of PCBP2, TAp73α, and actin were determined by Western blot analysis. The basal levels of TAp73α were arbitrarily set at 1.0, and the -fold change is shown *below each lane*.

SpectraMax GeminiXS Fluorometer (Molecular Devices) with excitation wavelength at 485 nm, emission wavelength at 538 nm, and cutoff at 530 nm. Triplicate samples were used for each experiment. Relative fluorescent units are the result of reading fluorescent units minus the background value and then divided by cell number.

Results

Knock-out or Knockdown of PCBP2 Decreased, Whereas Ectopic Expression of PCBP2 Increased TAp73 Expression—To determine whether PCBP2 regulates TAp73 expression, PCBP2 was knocked down by a PCBP2 siRNA in p53$^{-/-}$ HCT116 cells along with a scrambled siRNA as a control. We showed that upon knockdown of PCBP2, the level of TAp73 protein was markedly decreased (Fig. 1*A*). Similar results were found in H1299, Mia-PaCa2, and SW480 cells (Fig. 1, *B–D*). To verify this observation, we generated stable cell lines in which PCBP2 was knocked out by using the CRISPR-cas9 system (24). As expected, PCBP2 was absent in p53$^{-/-}$ HCT116, Mia-PaCa2, and H1299 cells (Fig. 1, *E–G*). Consistently, we found that the

levels of TAp73 protein were markedly decreased in PCBP2-knock-out (PCBP2-KO) cells as compared with that in parental cells (Fig. 1, *E–G*). To verify this, a vector expressing PCBP2 was transiently transfected into PCBP2-KO p53$^{-/-}$ HCT116, Mia-PaCa2, and H1299 cells along with an empty vector as a control. We showed that ectopic expression of PCBP2 led to increased expression of TAp73 in all three cell lines (Fig. 1, *H–J*). Together, these data suggest that PCBP2 regulates TAp73 expression.

PCBP2 Regulates TAp73 Expression via mRNA Stability— RNA-binding proteins are known to regulate their targets through posttranscriptional mechanisms including mRNA stability. Thus, to explore how PCBP2 regulates TAp73 expression, p53$^{-/-}$ HCT116 cells were transfected with a scrambled or PCBP2 siRNA, and the level of TAp73 transcripts was measured by qRT-PCR. We found that upon knockdown of PCBP2, the level of TAp73 transcripts was decreased in p53$^{-/-}$ HCT116 cells (Fig. 2*A*). Similarly, the level of TAp73 transcripts was down-regulated by knockdown of PCBP2 in H1299, Mia-PaCa2, and SW480 cells (Fig. 2, *B–D*). Moreover, we found that
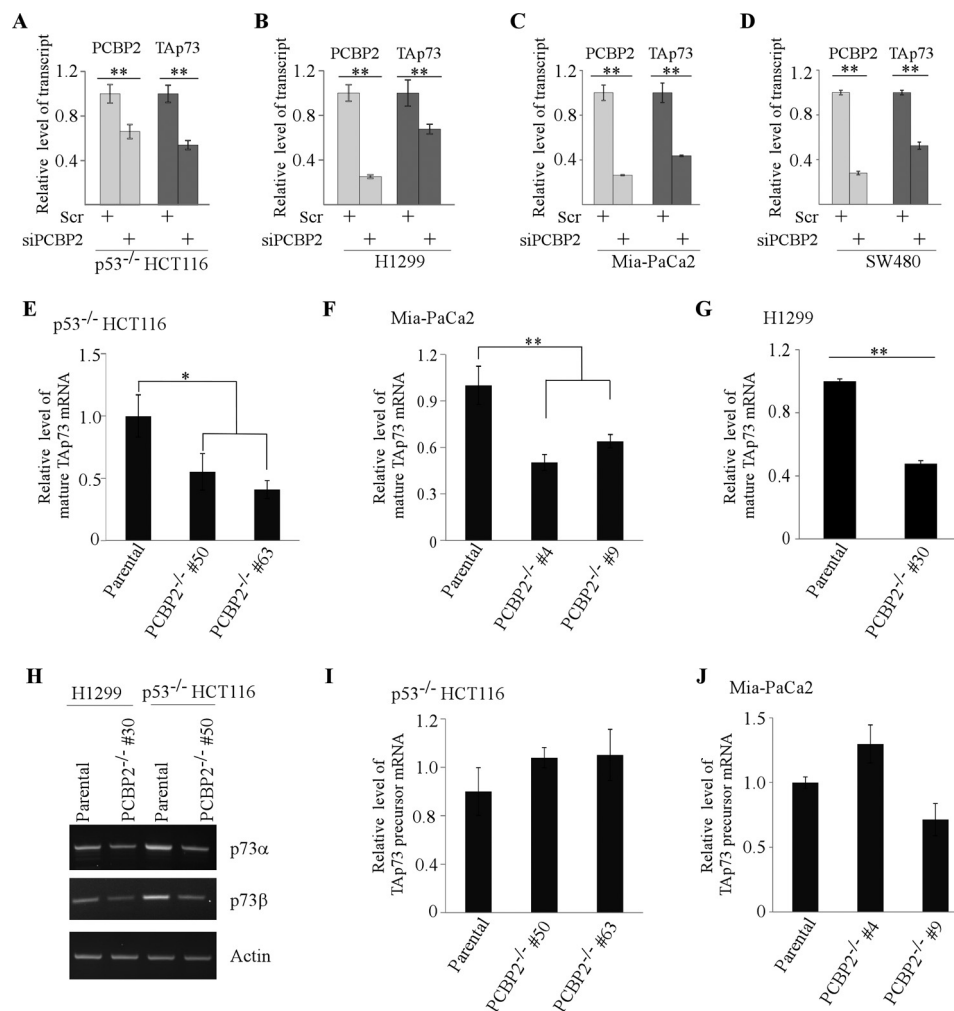
FIGURE 2. **The level of p73 transcripts was decreased upon knockdown or knock-out of PCBP2.** *A–D*, p53$^{-/-}$ HCT116 (*A*), H1299 (*B*), Mia-PaCa2 (*C*), and SW480 (*D*) cells were transiently transfected with a scrambled or PCBP2siRNA for 3 days followed by qRT-PCR to measure the level of PCBP2 and TAp73 transcripts. *E–G*, the levels of TAp73 transcripts were determined by qRT-PCR in parental and PCBP2-KO p53$^{-/-}$ HCT116 (*E*), Mia-PaCa2 (*F*), and H1299 (*G*) cells. *H*, the levels of p73α and p73β transcripts were determined by RT-PCR in parental and PCBP2-KO H1299 and p53$^{-/-}$ HCT116 cells. *I–J*, the levels of TAp73 precursor mRNA were determined by qRT-PCR in parental and PCBP2-KO p53$^{-/-}$ HCT116 (*I*) and Mia-PaCa2 (*J*). All data are presented as the mean ± S.D. *, *p* < 0.05 and **, *p* < 0.01 by Student's *t* test).

knock-out of PCBP2 significantly reduced the level of TAp73 transcripts in p53$^{-/-}$ HCT116, Mia-PaCa2, and H1299 cells (Fig. 2, *E–G*). Additionally, we found that the level of p73α and p73β transcripts was reduced upon knock-out of PCBP2 (Fig. 2*H*). In contrast, the level of TAp73 precursor mRNA was not altered by knock-out of PCBP2 (Fig. 2, *I–J*), suggesting that PCBP2 posttranscriptionally regulates TAp73 expression, likely via mRNA stability.

Next, to examine whether PCBP2 regulates p73 mRNA decay, the half-life of TAp73 transcripts was determined in parental and PCBP2-KO p53$^{-/-}$ HCT116 cells treated with 5,6-dichlorobenzimidazole 1-β-D-ribofuranoside, an inhibitor of *de novo* transcription. We showed that the half-life of p73 transcripts was 4.9 h in parental p53$^{-/-}$ HCT116 cells, which was reduced to 3.8 h in PCBP2-KO p53$^{-/-}$ HCT116 cells (Fig. 3*A*). Consistent with this, we showed that knockdown of PCBP2 reduced the half-life of p73 transcripts from 6.2 h to 4.5 h in H1299 cells (Fig. 3*B*). Together, these data suggest that PCBP2 is necessary for p73 mRNA stability. We note that the half-life of TAp73 transcripts was moderately longer in H1299
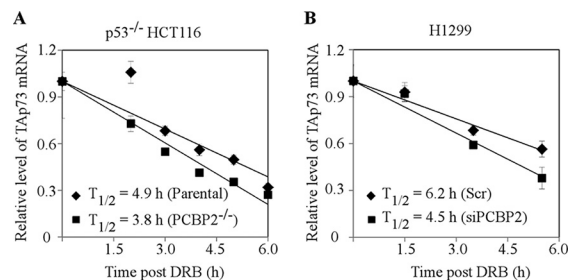

FIGURE 3. **PCBP2 regulated p73 expression via mRNA stability.** *A*, the half-life of p73 transcripts was decreased by loss of PCBP2. Parental and PCBP2-KO p53$^{-/-}$ HCT116 cells were treated with 5, 6-dichloro-1-β-D-ribofuranosyl-benzimidazole (*DRB*) for the indicated times. The relative level of TAp73 transcripts was normalized to actin and presented as the mean ± S.D. from triplicate samples. The relative level of the remaining mRNA was plotted over time, and the half-life of TAp73 transcript was calculated. *B*, the experiment was performed as in *A* except that H1299 cells were transiently transfected with scrambled or PCBP2 siRNA for 3 days.

cells (~6.2 h) than that in p53$^{-/-}$ HCT116 cells (~4.9 h), likely due to other p73 modulators that are differentially expressed in these two cell lines.
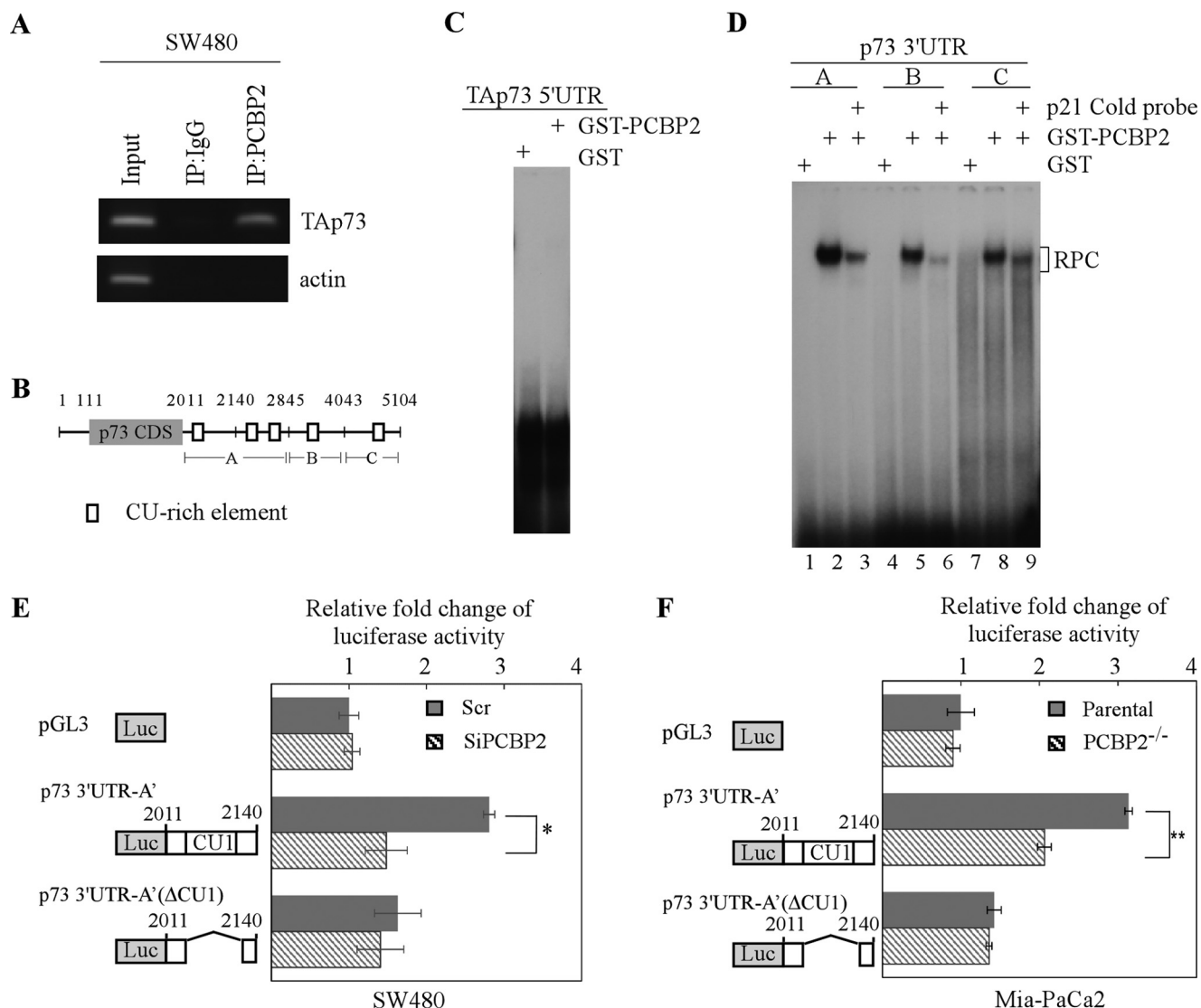
FIGURE 4. **The CU-rich element in p73 3′-UTR is bound by PCBP2 and is necessary for p73 mRNA stability.** *A*, SW480 cell lysates were immunoprecipitated (*IP*) with a control IgG or anti-PCBP2. TAp73 and actin transcripts in the immunocomplexes were analyzed by RT-PCR using specific primers for TAp73 and actin. *B*, schematic presentation of TAp73α transcript and the locations of CU-rich elements and probes used for REMSA. *C*, PCBP2 did not bind to TAp73 5′-UTR. REMSA was performed as described under "Materials and Methods" using recombinant GST or GST-fused PCBP2 along with ^{32}P-labeled TAp73 5′-UTR probe. *D*, PCBP2 binds to p73 3′-UTR. REMSA was performed as in *C* with ^{32}P-labeled RNA probes derived from p73 3′-UTR (fragments *A*, *B*, and *C*). For the competition assay, 50-fold of unlabeled p21 probe was added to the reaction. *RPC* indicates RNA-protein complexes. *E*, *left panel*, schematic presentation of a control pGL3 reporter or a luciferase reporter containing partial p73 3′-UTR along with or without CU1 deletion. *Right panel*, SW480 cells was transfected with a scrambled or PCBP2 siRNA for 2 days and then transfected with a control pGL3 reporter, p73 3′-UTR-A′, or p73 3′-UTR-A′ (ΔCU1) luciferase reporter for 24 h. The luciferase assay was performed as described under "Materials and Methods." Data were presented as the mean ± S.D. from triplicate samples (*, $p < 0.05$ by Student's *t* test). *F*, parental and PCBP2-KO Mia-PaCa2 were used for luciferase assay as described in *E*. Data were presented as the mean ± S.D. from triplicate samples (**, $p < 0.01$ by Student's *t* test).

CU-rich Elements in p73 3′-UTR Are Bound by PCBP2 and Are Necessary for p73 mRNA Stability—To explore the mechanism by which PCBP2 stabilizes p73 mRNA, RNA immunoprecipitation followed by RT-PCR was performed to determine whether PCBP2 associates with p73 transcripts. We found that in SW480 cells, TAp73 mRNA was detected in the PCBP2-, but not in control IgG-, immunocomplexes (Fig. 4*A*, *TAp73 panel*), suggesting that PCBP2 is associated with p73 transcripts. As a control, actin mRNA was not detected in anti-PCBP2 immunocomplexes (Fig. 4*A*, *actin panel*). Because PCBP2-binding sites are CU-rich (34), we searched for potential CU-rich elements in p73 transcript. Indeed, several CU-rich elements were found in the 3′-UTR of p73 mRNA (Fig. 4*B*). Next, to map the PCBP2-

binding site(s), REMSA was performed with radiolabeled RNA probes derived from p73 5′-UTR and 3′-UTR (fragment A, B, and C) (Fig. 4*B*). We found that PCBP2 was unable to bind to p73 5′-UTR (Fig. 4*C*). However, recombinant GST-tagged PCBP2, but not GST protein, formed a complex with probe A, B, and C, with probe A exhibiting the strongest binding affinity (Fig. 4*D*, *lanes 2*, *5*, and *8*). Moreover, the binding of PCBP2 with probes A-C was inhibited by adding cold p21 probe (Fig. 4*D*, *lanes 3*, *6*, and *9*). We note that p21 3′-UTR contains a known PCBP2-binding site (13).

As probe A exhibits a strong affinity to PCBP2 (Fig. 4*D*), we therefore sought to examine whether the first CU-rich element (CU1) in fragment A is responsive to PCBP2 *in vivo*. In this

regard, we utilized two luciferase reporters that were previously generated (26). The first luciferase reporter, called p73 3′-UTR-A′, had an intact CU1, whereas the second luciferase reporter, called p73 3′-UTR-A′ (ΔCU1), did not contain CU1 (Fig. 4*E*, *left panel*). Next, SW480 cells were transfected with a scrambled siRNA (Scr) or a siRNA against PCBP2 for 2 days followed by transfection with a control pGL3 vector, p73 3′-UTR-A′, or p73 3′-UTR-A′ (ΔCU1). We showed that the luciferase activity for p73 3′-UTR-A′ was markedly reduced in PCBP2-KD cells from that in PCBP2-competent cells (Fig. 4*E*, *right panel*). By contrast, the luciferase activity for pGL3 and p73 3′-UTR-A′ (ΔCU1) was not decreased by PCBP2 knockdown (Fig. 4*E*, *right panel*). Similarly, we showed that the luciferase activity for p73 3′-UTR-A′ was markedly decreased by knock-out of PCBP2 in Mia-PaCa2 cells (Fig. 4*F*). Together, these data suggest that the CU-rich element in p73 3′-UTR is critical for PCBP2 to regulate p73 mRNA stability. We note that in PCBP2$^{-/-}$ Mia-PaCa2 cells the level of luciferase activity for p73 3′-UTR-A′ was slightly higher than that for p73 3′-UTR-A′ (ΔCU1) (Fig. 4*F*), suggesting that another p73 modulator(s) may play a role in p73 expression.

PCBP2 Regulates ROS Production via TAp73 and Its Target Glutaminase-2 (GLS2)—TAp73 is known to regulate intracellular ROS production (4), a crucial factor for both cancer and aging (35). Thus, to determine the biological significance of PCBP2-mediated p73 expression, ROS production was measured in parental and PCBP2-KO H1299 and Mia-PaCa2 cells. We found that upon knock-out of PCBP2, the level of ROS was increased in both H1299 and Mia-PaCa2 cells (Fig. 5, *A* and *B*). Conversely, ectopic expression of PCBP2 reduced the level of ROS in PCBP2-KO H1299 cells (Fig. 5*C*). Next, we examined whether increased ROS production induced by lack of PCBP2 can be reduced by TAp73. We found that upon ectopic expression of TAp73α (Fig. 5*D*, *left panel*), ROS accumulation induced by loss of PCBP2 was suppressed (Fig. 5*D*, *right panel*). To verify this, ROS production was determined in parental and TAp73-KO H1299 cells along with or without PCBP2 knockdown. We showed that knockdown of PCBP2 increased ROS production in parental H1299 cells (Fig. 5*E*). However, knockdown of PCBP2 was unable to further increase ROS production in the absence of TAp73 (Fig. 5*E*). Together, these data suggest that loss of PCBP2 leads to decreased expression of TAp73 and, subsequently, increased production of ROS.

GLS2, a p53 target gene, is found to play a role in antioxidant defense by increasing reduced glutathione and by decreasing ROS production (36). Recent studies also showed that GLS2 is regulated by TAp73 and involved in TAp73-mediated ROS production (37). Thus, we examined whether GLS2 expression is altered by PCBP2. To rule out the potential interference of p53, p53-null H1299 cells were used. We found that upon knock-out of PCBP2 in H1299 cells, GLS2 expression was significantly decreased (Fig. 5*F*). Consistent with this, we showed that ectopic expression of PCBP2 led to increased expression of GLS2 in H1299 cells (Fig. 5*G*). Together, these data suggest that PCBP2 modulates ROS production via TAp73 and its target, GLS2.
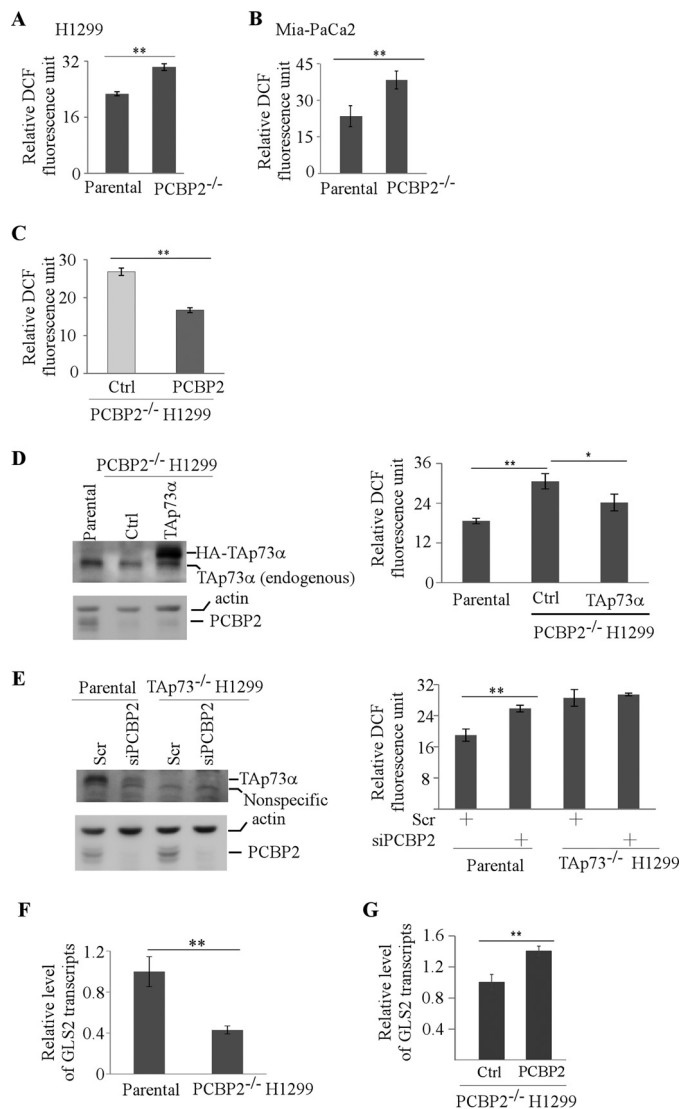

FIGURE 5. **PCBP2 regulates ROS production via TAp73 and its target GLS2.** *A* and *B*, the level of ROS was measured in parental and PCBP2-KO H1299 (*A*) and Mia-PaCa2 (*B*) cells by 2′,7′-dichlorofluorescin diacetate (*DCF*) staining using a microplate reader. Relative fluorescence units are calculated by subtracting the background value and then divided by cell number. Data were presented as the mean ± S.D. from triplicate samples (**, $p < 0.01$ by Student's *t* test). *C*, the level of ROS was determined in PCBP2-KO H1299 cells transiently transfected with a control or PCBP2-expressing vector. *D*, ectopic expression of TAp73α reduced ROS production induced by loss of PCBP2. *Left panel*, the levels of TAp73α, PCBP2, and actin were determined in parental H1229 cells and PCBP2-KO H1299 cells transiently transfected with a control or TAp73α-expressing vector. *Right panel*, the level of ROS was measured using cells treated as in the *left panel*. Data are presented as the mean ± S.D. from triplicate samples (, *$p < 0.05$ and **, $p < 0.01$ by Student's *t* test). *E*, PCBP2 was unable to regulate ROS production in the absence of TAp73. *Left panel*, the levels of TAp73α, PCBP2, and actin were determined in parental and TAp73-KO H1299 cells transiently transfected with a scrambled or PCBP2 siRNA for 3 days. *Right panel*, the level of ROS was measured using cells treated as in the *left panel*. Data are presented as the mean ± S.D. from triplicate samples (**, $p < 0.01$ by Student's *t* test). *F*, the level of GLS2 transcripts was determined by qRT-PCR in parental and PCBP2-KO H1299 cells. Data are presented as the mean ± S.D. from triplicate samples (**, $p < 0.01$ by Student's *t* test). *G*, the level of GLS2 transcripts was determined in PCBP2-KO H1299 cells transiently transfected with a control or PCBP2-expressing vector. Data are presented as the mean ± S.D. from triplicate samples (*, $p < 0.5$ and **, $p < 0.01$ by Student's *t* test).

Loss of PCBP2 Leads to ROS Accumulation and Accelerated Cellular Senescence in Primary MEFs—Aberrant production of ROS is associated with accelerated cellular senescence (38).
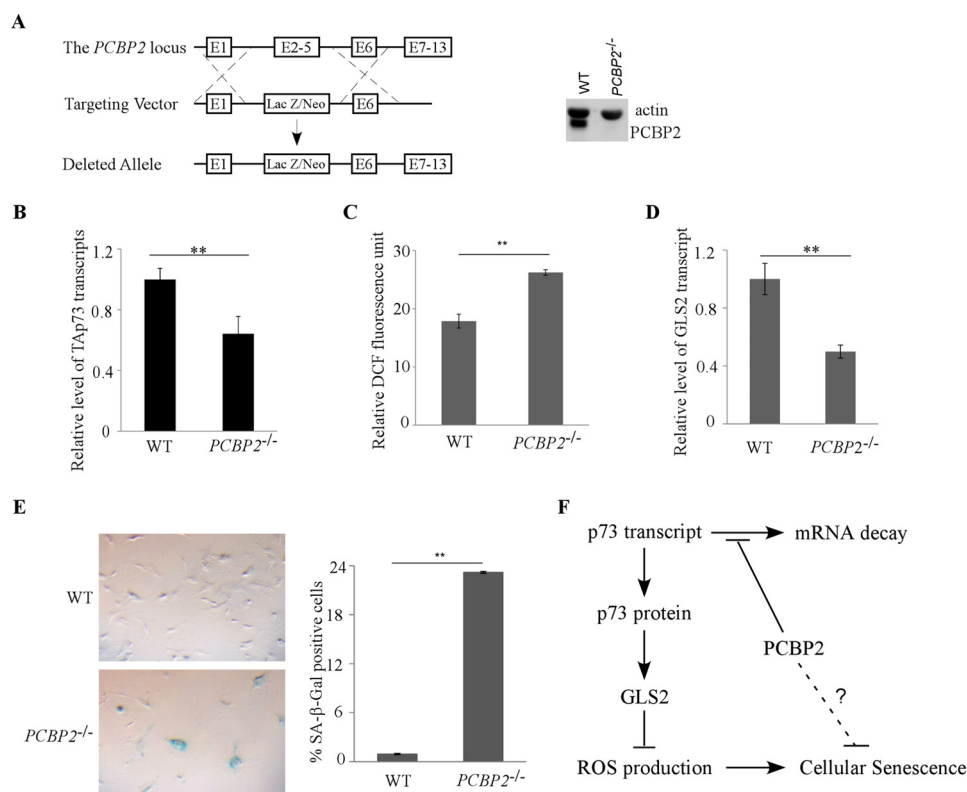
FIGURE 6. **Loss of PCBP2 leads to ROS accumulation and accelerated cellular senescence in primary MEFs.** *A*, *left panel*, schematic representation of the strategy to generate *PCPB2*$^{-/-}$ mouse. *Right panel*, the level of PCBP2 and actin was measured in wild-type and *PCBP2*$^{-/-}$ MEFs by Western blot analysis. *B*, the level of TAp73 transcripts was determined by qRT-PCR using wild-type and *PCBP2*$^{-/-}$ MEFs. **, $p < 0.01$ by Student's *t* test. *C*, the level of ROS was measured in wild-type and *PCBP2*$^{-/-}$ MEFs. **, $p < 0.01$ by Student's *t* test. *D*, the level of GLS2 transcripts in wild-type and *PCBP2*$^{-/-}$ MEFs was determined by qRT-PCR. **, $p < 0.01$ by Student's *t* test. *E*, *left panel*, representative images of SA-β-gal stained wild-type and *PCBP2*$^{-/-}$ MEFs. *Right panel*, quantification of the percentage of SA-β-gal-positive cells as shown in the *left panel*. **, $p < 0.01$ by Student's *t* test. *F*, a model for the role of PCBP2 in TAp73 expression, ROS production, and cellular senescence.

Thus, we sought to determine whether PCBP2-mediated ROS production has any effect on cellular senescence in primary MEFs. In this regard, we generated wild-type and *PCBP2*$^{-/-}$ MEFs by intercrossing *PCBP2*$^{+/-}$ mice (Fig. 6*A*). We showed that the level of TAp73 transcript was decreased in *PCBP2*$^{-/-}$ MEFs as compared with that in WT MEFs (Fig. 6*B*), consistent with the data obtained in human cells (Fig. 2). We also showed that loss of *PCBP2* led to increased production of ROS in MEFs (Fig. 6*C*). Moreover, we found that loss of *PCBP2* led to decreased expression of GLS2 in MEFs (Fig. 6*D*). Next, SA-β-gal staining assay was performed to measure the effect of PCBP2-deficiency on cellular senescence. We found that the number of cells stained positive with SA-β-gal was markedly increased in *PCBP2*$^{-/-}$ MEFs as compared with that in wild-type MEFs (Fig. 6*E*). Together, these data suggest that loss of PCBP2 leads to an increase in ROS production and possibly, cellular senescence.

Discussion

Due to its critical role in tumor suppression and neuronal development, p73 has been subjected to extensive investigation. However, very little is known about how p73 expression is controlled by RNA-binding proteins at the posttranscriptional level. In the current study we showed that TAp73 expression is regulated by PCBP2 RNA-binding protein via mRNA stability. We also showed that PCBP2-regulated TAp73 expression is

critical for controlling ROS production at least in part via GLS2, a p73 target. Furthermore, we showed that loss of PCBP2 leads to decreased TAp73 expression in MEFs, which is accompanied by ROS accumulation and accelerated cellular senescence. Based on these findings, a model was proposed and presented in Fig. 6*F*.

In our study we showed that PCBP2 regulates p73 expression via mRNA stability. However, it is still not clear how PCBP2 stabilizes p73 mRNA. It is possible that PCBP2 might facilitate the transportation of p73 mRNA from nucleus to cytosol wherein protein is translated. Additionally, PCBP2 might protect p73 transcripts from degradation by cytoplasmic mRNA degradation complex. Therefore, further studies are warranted to address these questions.

To date, only a few RNA-binding proteins are found to regulate p73 expression. In addition to PCPB2 (this study), p73 expression is found to be regulated by Rbm38 RNA-binding protein via mRNA stability (26). Interestingly, Rbm38 also binds to the CU-rich elements in p73 3′-UTR (26). Apart from RNA-binding proteins, TAp73 expression is found to be repressed by miR-193 (39). Additionally, p73 is involved in microRNA-processing (40) and regulates several microRNAs including microRNA-34a (41). Therefore, it will be interesting to determine whether PCBP2 can collaborate or antagonize with other RNA-binding proteins or microRNAs to regulate

p73 expression and how these regulations affect p73 biological function.

We showed that PCBP2 modulates ROS production via GLS2 in a TAp73-dependent manner (Figs. 5, *D–G*, and 6*D*). We also showed that loss of *PCBP2* in primary MEFs led to increased production of ROS and accelerated cellular senescence (Fig. 6*E*). Together, these data suggest that PCBP2-regulated TAp73 expression is critical for proper production of ROS and normal cell proliferation. However, several questions remain to be addressed. First, PCBP2 regulates iron homeostasis, which is also known to be associated with cellular senescence (42). Thus, it is possible that PCBP2 can regulate cellular senescence independent of p73. Second, we note that the increased ROS production and cellular senescence are conserved between $PCBP2^{-/-}$ (this study) and $TAp73^{-/-}$ MEFs (4). Thus, it will be interesting to determine whether PCBP2 regulates p73-dependent activity *in vivo* by using *PCBP2* and *p73* compound mice. Third, in addition to GLS2, several other p73 targets, including glucose-6-phosphate dehydrogenase (43) and cytochrome *c* oxidase subunit 4 (Cox4i1) (4), are found to regulate ROS production and cellular senescence. Fourth, in addition to p73, PCBP2 may regulate p53 and p63, two other p53 family members. Thus, it will be interesting to determine whether PCBP2 regulates other p53 family members along with glucose-6-phosphate dehydrogenase and cytochrome *c* oxidase subunit 4 and how these regulations affect the activities of the p53 family tumor suppressors. Addressing these questions may unravel a cross-talk between the p53 family and PCBP family, which may be helpful for the development of novel strategy for cancer management.

References

1. Murray-Zmijewski, F., Lane, D. P., and Bourdon, J. C. (2006) p53/p63/p73 isoforms: an orchestra of isoforms to harmonise cell differentiation and response to stress. *Cell Death Differ.* **13**, 962–972
2. Harms, K., Nozell, S., and Chen, X. (2004) The common and distinct target genes of the p53 family transcription factors. *Cell. Mol. Life Sci.* **61**, 822–842
3. Tomasini, R., Tsuchihara, K., Wilhelm, M., Fujitani, M., Rufini, A., Cheung, C. C., Khan, F., Itie-Youten, A., Wakeham, A., Tsao, M. S., Iovanna, J. L, Squire, J., Jurisica, I., Kaplan, D., Melino, G., *et al.* (2008) TAp73 knockout shows genomic instability with infertility and tumor suppressor functions. *Genes Dev.* **22**, 2677–2691
4. Rufini, A., Niklison-Chirou, M. V., Inoue, S., Tomasini, R., Harris, I. S., Marino, A., Federici, M., Dinsdale, D., Knight, R. A., Melino, G., and Mak, T. W. (2012) TAp73 depletion accelerates aging through metabolic dysregulation. *Genes Dev.* **26**, 2009–2014
5. Kartasheva, N. N., Contente, A., Lenz-Stöppler, C., Roth, J., and Dobbelstein, M. (2002) p53 induces the expression of its antagonist p73ΔN, establishing an autoregulatory feedback loop. *Oncogene*, **21**, 4715–4727
6. Nakagawa, T., Takahashi, M., Ozaki, T., Watanabe Ki, K., Todo, S., Mizuguchi, H., Hayakawa, T., and Nakagawara, A. (2002) Autoinhibitory regulation of p73 by ΔNp73 to modulate cell survival and death through a p73-specific target element within the ΔNp73 promoter. *Mol. Cell. Biol.* **22**, 2575–2585
7. Petrenko, O., Zaika, A., and Moll, U. M. (2003) ΔNp73 facilitates cell immortalization and cooperates with oncogenic Ras in cellular transfor-

8. Wilhelm, M. T., Rufini, A., Wetzel, M. K., Tsuchihara, K., Inoue, S., Tomasini, R., Itie-Youten, A., Wakeham, A., Arsenian-Henriksson, M., Melino, G., Kaplan, D. R., Miller, F. D., and Mak, T. W. (2010) Isoform-specific p73 knockout mice reveal a novel role for ΔNp73 in the DNA damage response pathway. *Genes Dev.* **24**, 549–560
9. Tissir, F., Ravni, A., Achouri, Y., Riethmacher, D., Meyer, G., and Goffinet, A. M. (2009) ΔNp73 regulates neuronal survival *in vivo*. *Proc. Natl. Acad. Sci. U.S.A.* **106**, 16871–16876
10. Makeyev, A. V., and Liebhaber, S. A. (2002) The poly(C)-binding proteins: a multiplicity of functions and a search for mechanisms. *RNA* **8**, 265–278
11. Kiledjian, M., Wang, X., and Liebhaber, S. A. (1995) Identification of two KH domain proteins in the α-globin mRNP stability complex. *EMBO J.* **14**, 4357–4364
12. Han, W., Xin, Z., Zhao, Z., Bao, W., Lin, X., Yin, B., Zhao, J., Yuan, J., Qiang, B., and Peng, X. (2013) RNA-binding protein PCBP2 modulates glioma growth by regulating FHL3. *J. Clin. Invest.* **123**, 2103–2118
13. Waggoner, S. A., Johannes, G. J., and Liebhaber, S. A. (2009) Depletion of the poly(C)-binding proteins αCP1 and αCP2 from K562 cells leads to p53-independent induction of cyclin-dependent kinase inhibitor (CDKN1A) and G_1 arrest. *J. Biol. Chem.* **284**, 9039–9049
14. Evans, J. R., Mitchell, S. A., Spriggs, K. A., Ostrowski, J., Bomsztyk, K., Ostarek, D., and Willis, A. E. (2003) Members of the poly (rC) binding protein family stimulate the activity of the c-myc internal ribosome entry segment *in vitro* and *in vivo*. *Oncogene* **22**, 8012–8020
15. Sean, P., Nguyen, J. H., and Semler, B. L. (2008) The linker domain of poly(rC) binding protein 2 is a major determinant in poliovirus cap-independent translation. *Virology* **378**, 243–253
16. Sean, P., Nguyen, J. H., and Semler, B. L. (2009) Altered interactions between stem-loop IV within the 5′ noncoding region of coxsackievirus RNA and poly(rC) binding protein 2: effects on IRES-mediated translation and viral infectivity. *Virology* **389**, 45–58
17. Rieder, E., Xiang, W., Paul, A., and Wimmer, E. (2003) Analysis of the cloverleaf element in a human rhinovirus type 14/poliovirus chimera: correlation of subdomain D structure, ternary protein complex formation and virus replication. *J. Gen. Virol.* **84**, 2203–2216
18. Deleted in proof
19. Leidgens, S., Bullough, K. Z., Shi, H., Li, F., Shakoury-Elizeh, M., Yabe, T., Subramanian, P., Hsu, E., Natarajan, N., Nandal, A., Stemmler, T. L., and Philpott, C. C. (2013) Each member of the poly-r(C)-binding protein 1 (PCBP) family exhibits iron chaperone activity toward ferritin. *J. Biol. Chem.* **288**, 17791–17802
20. Frey, A. G., Nandal, A., Park, J. H., Smith, P. M., Yabe, T., Ryu, M. S., Ghosh, M. C., Lee, J., Rouault, T. A., Park, M. H., and Philpott, C. C. (2014) Iron chaperones PCBP1 and PCBP2 mediate the metallation of the dinuclear iron enzyme deoxyhypusine hydroxylase. *Proc. Natl. Acad. Sci. U.S.A.* **111**, 8031–8036
21. Nandal, A., Ruiz, J. C., Subramanian, P., Ghimire-Rijal, S., Sinnamon, R. A., Stemmler, T. L., Bruick, R. K., and Philpott, C. C. (2011) Activation of the HIF prolyl hydroxylase by the iron chaperones PCBP1 and PCBP2. *Cell Metab.* **14**, 647–657
22. Perrotti, D., and Calabretta, B. (2002) Post-transcriptional mechanisms in BCR/ABL leukemogenesis: role of shuttling RNA-binding proteins. *Oncogene* **21**, 8577–8583
23. Roychoudhury, P., Paul, R. R., Chowdhury, R., and Chaudhuri, K. (2007) HnRNP E2 is down-regulated in human oral cancer cells and the overexpression of hnRNP E2 induces apoptosis. *Mol. Carcinog.* **46**, 198–207
24. Ran, F. A., Hsu, P. D., Wright, J., Agarwala, V., Scott, D. A., and Zhang, F. (2013) Genome engineering using the CRISPR-Cas9 system. *Nat. Protoc.* **8**, 2281–2308
25. Liu, G., and Chen, X. (2005) The C-terminal sterile α motif and the extreme C terminus regulate the transcriptional activity of the α isoform of p73. *J. Biol. Chem.* **280**, 20111–20119
26. Yan, W., Zhang, J., Zhang, Y., Jung, Y. S., and Chen, X. (2012) p73 expression is regulated by RNPC1, a target of the p53 family, via mRNA stability. *Mol. Cell. Biol.* **32**, 2336–2348
27. Ghosh, D., Srivastava, G. P., Xu, D., Schulz, L. C., and Roberts, R. M. (2008) A link between SIN1 (MAPKAP1) and poly(rC) binding protein 2 (PCBP2)

in counteracting environmental stress. *Proc. Natl. Acad. Sci. U.S.A.* **105,** 11673–11678

28. Cho, S. J., Jung, Y. S., Zhang, J., and Chen, X. (2012) The RNA-binding protein RNPC1 stabilizes the mRNA encoding the RNA-binding protein HuR and cooperates with HuR to suppress cell proliferation. *J. Biol. Chem.* **287,** 14535–14544

29. Ren, C., Cho, S. J., Jung, Y. S., and Chen, X. (2014) DNA polymerase eta is regulated by poly(rC)-binding protein 1 via mRNA stability. *Biochem. J.* **464,** 377–386

30. Zhang, J., Xu, E., and Chen, X. (2013) Regulation of Mdm2 mRNA stability by RNA-binding protein RNPC1. *Oncotarget* **4,** 1121–1122

31. Lei, Y. (2013) Generation and culture of mouse embryonic fibroblasts. *Methods Mol. Biol.* **1031,** 59–64

32. Qian, Y., Zhang, J., Yan, B., and Chen, X. (2008) DEC1, a basic helix-loop-helix transcription factor and a novel target gene of the p53 family, mediates p53-dependent premature senescence. *J. Biol. Chem.* **283,** 2896–2905

33. Rosenkranz, A. R., Schmaldienst, S., Stuhlmeier, K. M., Chen, W., Knapp, W., and Zlabinger, G. J. (1992) A microplate assay for the detection of oxidative products using 2′,7′-dichlorofluorescin diacetate. *J. Immunol. Methods* **156,** 39–45

34. Ostareck-Lederer, A., Ostareck, D. H., and Hentze, M. W. (1998) Cytoplasmic regulatory functions of the KH-domain proteins hnRNPs K and E1/E2. *Trends Biochem. Sci.* **23,** 409–411

35. Afanas'ev, I. (2011) Reactive oxygen species signaling in cancer: comparison with aging. *Aging Dis.* **2,** 219–230

36. Suzuki, S., Tanaka, T., Poyurovsky, M. V., Nagano, H., Mayama, T., Ohkubo, S., Lokshin, M., Hosokawa, H., Nakayama, T., Suzuki, Y., Sugano, S., Sato, E., Nagao, T., Yokote, K., Tatsuno, I., and Prives, C. (2010) Phosphate-activated glutaminase (GLS2), a p53-inducible regulator of glutamine metabolism and reactive oxygen species. *Proc. Natl. Acad. Sci. U.S.A.* **107,** 7461–7466

37. Velletri, T., Romeo, F., Tucci, P., Peschiaroli, A., Annicchiarico-Petruzzelli, M., Niklison-Chirou, M., Amelio, I., Knight, R., Mak, T., Melino, G., and Agostini, M. (2015) GLS2 is transcriptionally regulated by p73 and contributes to neuronal differentiation. *Cell Cycle* **14,** 1611–1612

38. Lu, T., and Finkel, T. (2008) Free radicals and senescence. *Exp. Cell Res.* **314,** 1918–1922

39. Ory, B., Ramsey, M. R., Wilson, C., Vadysirisack, D. D., Forster, N., Rocco, J. W., Rothenberg, S. M., and Ellisen, L. W. (2011) A microRNA-dependent program controls p53-independent survival and chemosensitivity in human and murine squamous cell carcinoma. *J. Clin. Invest.* **121,** 809–820

40. Boominathan, L. (2010) The tumor suppressors p53, p63, and p73 are regulators of microRNA processing complex. *PLoS ONE* **5,** e10615

41. Agostini, M., Tucci, P., Killick, R., Candi, E., Sayan, B. S., Rivetti di Val Cervo, P., Nicotera, P., McKeon, F., Knight, R. A., Mak, T. W., and Melino, G. (2011) Neuronal differentiation by TAp73 is mediated by microRNA-34a regulation of synaptic protein targets. *Proc. Natl. Acad. Sci. U.S.A.* **108,** 21093–21098

42. Killilea, D. W., Atamna, H., Liao, C., and Ames, B. N. (2003) Iron accumulation during cellular senescence in human fibroblasts *in vitro*. *Antioxid. Redox Signal.* **5,** 507–516

43. Du, W., Jiang, P., Mancuso, A., Stonestrom, A., Brewer, M. D., Minn, A. J., Mak, T. W., Wu, M., and Yang, X. (2013) TAp73 enhances the pentose phosphate pathway and supports cell proliferation. *Nat. Cell Biol.* **15,** 991–1000